Composites Science and Technology 69 (2009) 186–191

Contents lists available at ScienceDirect

Composites Science and Technology

journal homepage: www.elsevier.com/locate/compscitech

Graphite oxide/poly(methyl methacrylate) nanocomposites prepared by a novel method utilizing macroazoinitiator

Jin Young Jang [a], Min Seok Kim [a], Han Mo Jeong [a,*], Cheol Min Shin [b]

[a] Department of Chemistry, University of Ulsan, San-29, Mugeo-dong, Ulsan 680-749, Republic of Korea
[b] Research Center, N-Baro Tech Co., 974-1, Goyeon-ri, Ungchon-myon, Ulju-gun, Ulsan 689-871, Republic of Korea

ARTICLE INFO

Article history:
Received 17 June 2008
Received in revised form 28 August 2008
Accepted 29 September 2008
Available online 7 October 2008

Keywords:
A. Polymer-matrix composites
B. Electrical properties
B. Thermomechanical properties
D. X-ray diffraction
Graphite oxide

ABSTRACT

Graphite oxide (GO)/poly(methyl methacrylate) (PMMA) nanocomposites were prepared by a novel method utilizing macroazoinitiator (MAI). The MAI, which has a poly(ethylene oxide) (PEO) segment, was intercalated between the lamellae of GO to induce the inter-gallery polymerization of methyl methacrylate (MMA) and exfoliate the GO. The morphological, conductivity, thermal, mechanical and rheological properties of these nanocomposites were examined and compared with those of intercalated nanocomposites prepared by polymerization with the normal radical initiator, 2,2′-azobisisobutyronitrile. The improvement in conductivity by GO was more evident in exfoliated nanocomposites compared to that of intercalated nanocomposites. For example, a conductivity of 1.78×10^{-7} S/cm was attained in the exfoliated nanocomposite prepared with 2.5 parts GO per 100 parts MMA, which was about 50-fold higher than that of the intercalated nanocomposite. The thermal, mechanical and rheological properties also indicate that thin GO with a high aspect ratio is finely dispersed and effectively reinforced the PMMA matrix in both exfoliated and intercalated nanocomposites.

1. Introduction

Nanocomposites composed of polymer matrices with reinforcements of less than 100 nm in size have attracted considerable attention as advanced materials because many physical properties of matrix polymers, such as their mechanical, electrical, barrier, and flame-retarding properties can be substantially enhanced with small amounts of reinforcements compared to conventional composites [1,2]. Because these unique properties of polymer nanocomposites come from their peculiar phase morphologies of intercalation or exfoliation, which maximize interfacial contact between the matrix polymer and reinforcements, the fillers with high surface-to-volume ratio, for example, layered silicates such as montmorillonite, that are composed of stacks of parallel lamellae with a 1 nm thickness and a high aspect ratio are most commonly utilized [3].

Graphite oxide (GO), which is prepared by the oxidation of graphite, has a layered structure composed of parallel pseudo two-dimensional lamellaes. Each layer consists of randomly distributed unoxidized aromatic regions and six-member aliphatic regions attached with polar groups, such as hydroxyl, epoxide, ether, and carboxylate groups, as a result of oxidation [4–6]. GO is quite similar to montmorillonite in that it can have intercalated or exfoliated structures in the polymer matrix to create a nanocomposite [7–9]. In addition, GO can impart electric conductivity to polymers [10], and GO can be used as host material for the synthesis of conducting polymer intercalated nanocomposites [11–14].

Because exfoliated nanocomposites usually provide the best property enhancements due to a large interfacial area and homogeneous dispersion, many efforts have been devoted to design methods that improve the delamination of silicate layers in the polymer matrix. Polymerization in the galleries between the silicate layers can promote exfoliation because the growing polymer chain can push apart and eventually delaminate the silicate layers. Therefore, the initiator, or co-monomer, located in the gallery, which induces inter-gallery polymerization, can be utilized for exfoliation [15,16].

The polar functional groups attached to carbon sheets make GO hydrophilic [5,6]. Therefore, the dispersion of GO in the hydrophobic polymer matrix requires a large favorable enthalpic contribution to overcome this discrepancy in polarity, as well as the entropy loss required for the chain to diffuse into the gallery. Therefore, hydrophobic modification of GO [17,18], block or graft copolymers containing a block that is miscible with the matrix polymer and another block that is compatible with GO can be utilized for the favorable enthalpic contribution.

Because GO has a larger interlayer spacing (I_c) compared to graphite, as well as polar functional groups, hydrophilic polymers such as poly(ethylene oxide), poly(vinyl alcohol), poly(diallyldimethylammoniumchloride), poly(furfuryl alcohol) can be easily inserted into the gallery of GO to make intercalated nanocomposites [19–23].

* Corresponding author. Tel.: +82 52 259 2343; fax: +82 52 259 2348.
E-mail address: hmjeong@mail.ulsan.ac.kr (H.M. Jeong).

0266-3538/$ - see front matter © 2008 Elsevier Ltd. All rights reserved.
doi:10.1016/j.compscitech.2008.09.039

Since poly(ethylene oxide) (PEO) can be easily intercalated at the GO gallery [19,20], the macroazoinitiator (MAI) containing a PEO segment, as shown in the following chemical structure, can also be intercalated easily in the GO gallery. Therefore, it is anticipated that intercalated MAI can be utilized to prepare exfoliated nanocomposites by inducing inter-gallery radical polymerization of vinyl monomers, and the polymerized PEO-vinyl monomer multi-block copolymer will have an affinity to GO due to the presence of PEO block.

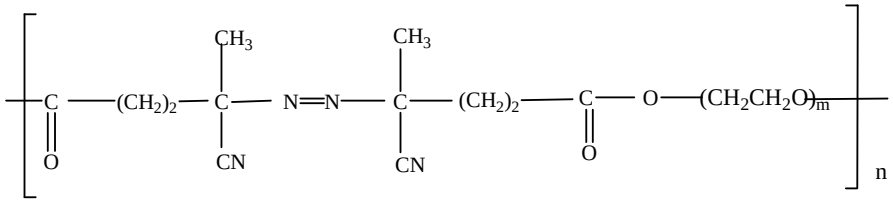

In the present study, we prepared exfoliated GO/poly(methyl methacrylate) (PMMA) nanocomposites with an MAI intercalated in the gallery of GO. The morphological, conductivity, thermal, and mechanical properties of these nanocomposites were examined and compared to those of nanocomposites prepared by normal radical polymerization with 2,2'-azobisisobutyronitrile (AIBN) as an initiator.

2. Experimental

2.1. Materials

Natural graphite (HC-598) with an average particle size of 11 μm was purchased from Hyundai Coma Co., Ltd. MAI (VPE-0201) was purchased from Wako Pure Chemical. It is the condensation polymer of 4,4′-azobis(4-cyanopentanoic acid) (ACPA) and poly(ethylene glycol) (molecular weight 2000) [24]. It has a molecular weight of about 22,000 and an azo group content of 0.45 mmol/g. MAI, methyl methacrylate (MMA, Aldrich), AIBN (Aldrich), acetonitrile (Aldrich), methanol (Aldrich), concentrated H_2SO_4 (96%, DC Chemical Co., Ltd.), $KMnO_4$ (Duksan Pure Chemical), H_2O_2 (30%, DC Chemical Co., Ltd.), and hydrochloric acid (35%, Daejung Chemicals & Metals Co., Ltd.) were used as received.

2.2. Preparation of GO

GO was prepared by oxidation with $KMnO_4/H_2SO_4$ [10]. In a typical experiment, $KMnO_4$ (15 g) was added slowly to a cooled 500 mL round-bottomed flask that contained conc. H_2SO_4 (110 mL) and graphite powder (10 g) with care that the reaction mixture be maintained below 20 °C, and the reaction mixture was stirred for 30 min at 30 °C. After slowly feeding distilled water (230 mL) into the reactor with care that the reaction mixture to be kept below 90 °C, the mixture was allowed to stir for another 30 min at 90 °C. To stop the oxidation reaction, additional distilled water (250 mL) and 30% H_2O_2 (20 mL), which reduced the excess $KMnO_4$, were fed sequentially into the reactor. The oxidized product, GO, was filtered, washed with 5% HCl aqueous solution several times and then with distilled water until neutralization, and dried in a vacuum oven at 50 °C for 24 h. Elemental analysis showed that the composition of GO was $C_{1.00}O_{0.23}H_{0.13}$.

2.3. Preparation of GO/PMMA nanocomposite

The GO intercalated with MAI (MAI/GO) was prepared using an acetonitrile/methanol mixture (1/1 by volume) as the solvent. After dissolving 0.10 g of MAI into 100 mL of the solvent, 0.50 g of GO was put into the solution and ultrasonic irradiation was applied for 30 min. Solid state MAI/GO was obtained by evaporation of the solvent at 25 °C under vacuum conditions.

The recipes for the preparation of GO/PMMA nanocomposites are shown in Table 1. In the case of Series A, bulk radical polymerization of MMA was carried out in the presence of GO with AIBN as an initiator under N_2 atmospheric conditions at 65 °C for 2 h while stirring with a magnetic bar. For the preparation of Series B, MAI/GO was swelled in a reactor with a 100-fold volume of water and then MMA was fed into the reactor while being stirred by a magnetic bar at room temperature. This heterogeneous system was heated to 65 °C to cause polymerization under N_2 atmospheric conditions for 5 h, and this was further polymerized for 1 h at 65 °C after feeding additional initiator, AIBN dissolved in MMA. The prepared GO/PMMA nanocomposites were crushed into powder and dried at 65 °C under vacuum conditions for 24 h to remove low molecular weight components.

2.4. Measurements

X-ray diffraction (XRD) patterns were obtained with an X-ray diffractometer (Rigaku, RAD-3C) using Cu K_α radiation (λ = 1.54 Å) as the X-ray source. The diffraction angle was scanned from 2° at a rate of 1.2°/min.

The morphology of nanocomposites was examined with a transmission electron microscope (TEM, Hitachi H-8100). Thin sections were cut perpendicularly to the nanocomposite fiber, which was extruded by a melt indexer at 240 °C. The acceleration voltage of TEM was 200 kV.

The direct current conductivity at room temperature across the 1 mm thick film, which was compression molded at 190 °C and a pressure of 22 MPa, was measured with a picoamperometer (Keithley 237) utilizing round-shaped silver electrodes measuring 0.28 cm^2 attached at both surfaces of the specimen. Silver paste was used to ensure good contact between the specimen surface and the electrode.

Table 1
Recipe for the preparation of GO/PMMA nanocomposites and polymerization yield.

Sample	Feed (by weight)				Concentration of azo group in feed (mmol/100 g-MMA)	Polymerization yield (%)
	MMA	AIBN	GO	MAI/GO		
Series A						
A-0	100	0.300	–	–	1.83	87.3
A-8	100	0.300	0.833	–	1.83	82.4
A-25	100	0.300	2.500	–	1.83	87.7
A-42	100	0.300	4.167	–	1.83	88.2
A-67	100	0.300	6.667	–	1.83	87.2
Series B						
B-8	100	0.288	–	0.167/0.833	1.83	86.6
B-17	100	0.275	–	0.333/1.667	1.83	84.5
B-25	100	0.263	–	0.500/2.500	1.83	80.7
B-33	100	0.251	–	0.667/3.333	1.83	86.4
B-42	100	0.239	–	0.833/4.167	1.83	85.6
B-50	100	0.226	–	1.000/5.000	1.83	87.4
B-67	100	0.202	–	1.333/6.667	1.83	84.7

Table 2
Physical properties of GO/PMMA nanocomposites.

Sample	Molecular weight		Conductivity (S/cm)	E' (MPa)		T_g (°C)		E'_f at 60 °C (GPa)	
	M_n	M_w		60 °C	190 °C	DMA	DSC	GO	MAI/GO
Series A									
A-0	60,623	214,292	Less than 10^{-14}	520	0.426	98.7	105.3	–	–
A-8	76,077	218,777	Less than 10^{-14}	679	0.712	121.1	115.7	16.4	–
A-25	90,072	235,220	3.48×10^{-9}	–	–	–	117.3	–	–
A-42	88,481	245,496	8.57×10^{-6}	903	1.031	122.2	117.4	9.0	–
A-67	103,388	275,886	5.65×10^{-5}	1139	2.289	128.0	119.5	9.2	–
Series B									
B-8	191,335	568,949	Less than 10^{-14}	569	1.551	107.6	116.0	–	4.7
B-17	133,191	434,121	1.64×10^{-14}	670	1.904	113.4	116.7	–	7.0
B-25	145,394	455,569	1.78×10^{-7}	–	–	–	117.4	–	–
B-33	159,772	455,092	1.09×10^{-7}	801	2.095	116.6	117.9	–	6.8
B-42	173,754	563,071	1.68×10^{-5}	903	2.333	119.5	118.9	–	7.4
B-50	151,482	618,537	2.10×10^{-5}	1030	2.858	120.3	119.1	–	8.4
B-67	131,673	477,954	8.26×10^{-4}	1160	3.239	114.6	122.6	–	7.8

The number average molecular weight (M_n) and weight average molecular weight (M_w) of PMMA were measured at 43 °C with gel permeation chromatography (GPC, Waters M510), and the results are shown in Table 2. The nanocomposite was dissolved in tetrahydrofuran (THF), and the solution was filtered with a 0.45 μm membrane filter before measurement. THF was used as an elutant.

Differential scanning calorimetry (DSC) was carried out with a DSC 823^e (Mettler Toledo) at a heating and cooling rate of 10 °C/min with 7 mg of sample. The samples stayed at 150 °C for 1 min in the DSC and were cooled down to 25 °C. The glass transition temperature (T_g) was measured in a subsequent heating scan.

Dynamic mechanical properties were determined using a dynamic mechanical analyzer (DMA, TA Instrument, DMA-Q800) with a bending mode at a heating rate of 5 °C/min and 1 Hz. Samples were compression molded at 190 °C and a pressure of 22 MPa.

3. Results and discussion

3.1. XRD and TEM

The diffractogram of pristine graphite (Fig. 1(a)) shows a very intense, sharp peak at $2\theta = 26.5°$ [5,25]. This peak corresponds to the diffraction of the (002) graphite plane composed of well-ordered graphenes with an interlayer spacing of $I_c = 3.35$ Å. In the diffractogram of GO (Fig. 1(b)), this peak becomes broader and smaller, and a new large and broader peak appears around $2\theta = 13.8°$, corresponding to the (002) plane of GO [4,5,25,26]. This shows that the I_c increased from 3.35 Å to about 6.4 Å by the oxidation because various functional groups were created on the surfaces of each GO layer. The small broad peak around $2\theta = 26°$ (Fig. 1(b)) shows that the crystal structure of graphite had not perfectly disappeared, but some amount of the structure, which was somewhat disturbed by mild oxidation, remained.

The X-ray diffraction pattern of MAI/GO (Fig. 1(c)) shows peaks at 9.5° and 19.2°, which correspond to the (002) and (004) reflections of MAI/GO. The migration of the (002) reflection peak to a lower angle ($2\theta = 9.5°$, $I_c = 9.3$ Å) compared to that of pristine GO ($2\theta = 13.8°$, $I_c = 6.4$ Å) (Fig 1(b)) and the presence of both (002) and (004) lines indicate the formation of a new intercalated compound. The small broad peak at $2\theta = 26°$ seems to be that of remaining graphite crystal whose structure was somewhat disturbed by mild oxidation. It was previously reported that the expansions of I_c are about 4 Å when a single layer of PEO was intercalated in a zig–zag conformation and about 8 Å when a single layer of PEO was intercalated in a helical chain conformation or a double layer of PEO was intercalated in a zig–zag conformation in the gallery of GO [19,20]. Compared to these values, the 2.9 Å (9.3–6.4 Å) expansion of I_c by the intercalation of MAI, as shown in Fig. 1, is smaller. Since water absorbed at the gallery can cause about 5 Å expansion of I_c [19,26], this small increase of I_c by the intercalation of MAI seems to be due to the complicated contribution of absorbed water molecules.

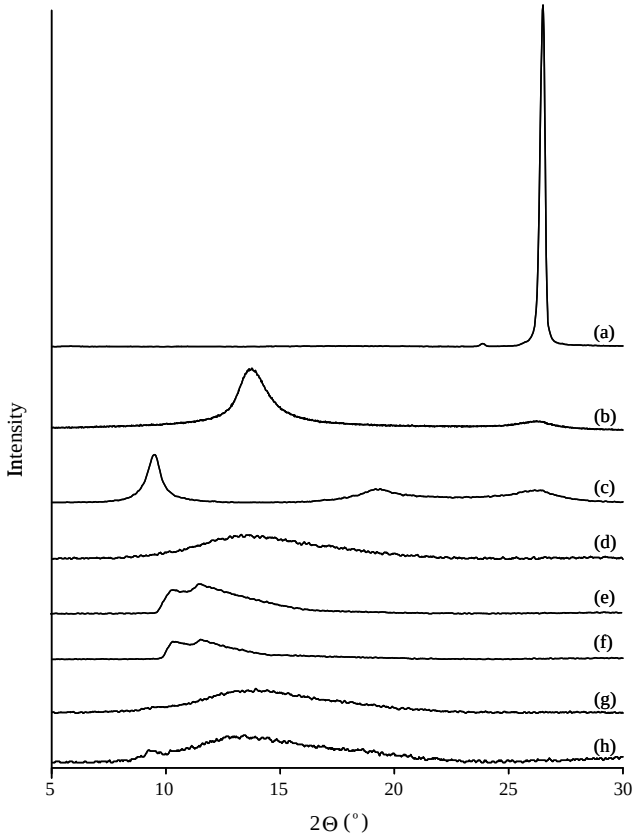

Fig. 1. XRD patterns of (a) graphite, (b) GO, (c) MAI/GO, (d) PMMA, (e) A-25, (f) A-67, (g) B-25, (h) B-67.

The series A compounds (Fig 1 (e) and (f)) have a broad XRD peak around $2\theta = 11°$ ($I_c = 8.0$ Å), which shows that the expansion of I_c by the intercalation of matrix molecules into the gallery of GO is about 1.6 Å, and the broad peak shape suggests that the I_c has a broad distribution due to various degrees of intercalation. However, the XRD patterns of Series B (Fig 1 (g) and (h)) do not show a peak of GO and are similar to that of PMMA (Fig 1 (d)).

These results show that each layer of GO is exfoliated in the PMMA matrix because in the exfoliated structure, where the individual GO layers are delaminated and randomly dispersed in the PMMA matrix, the distances between the GO layers are too far and the layers are too disordered to give a coherent wide-angle XRD signal at $2\theta > 2^\circ$ [15,27].

The TEM image of A-67 (Fig. 2 (a)) shows no particle-like material except flexible, wrinkled sheets of GO dispersed in the PMMA matrix [5,22,28]. However, one can observe black heterogeneous regions, which shows that there exist thick GOs composed of several GO sheets. In contrast, the TEM image of B-67 (Fig. 2(b)) shows that the GO sheets, whose transparency for electron beam is better compared to those of Fig. 2(a), are finely dispersed in the matrix of PMMA. This indicates that de-lamination of the GO sheets was effectively induced by the polymerization with MAI to yield an exfoliated GO/PMMA nanocomposite.

3.2. Physical properties

The highly oxidized GO is an insulating material [29,30], however, when moderately oxidized GO can have a proper electric conductivity that can be utilized as a conductive filler [10]. The GO used in this study has a conductivity of 0.5 S/cm because we prepared the GO by mild oxidation method [10]. In many papers [4–6,31], the C/O number ratios of GO are in the range of 2/1–3/1. However, GO used in this paper has the value of 4.35/1.00. This shows that this GO was moderately oxidized to have a proper electric conductivity. In the infrared (IR) spectrum, the ratio of percentage absorption at 1580 cm^{-1} to that at 1234 cm^{-1} can give the information about the degree of GO oxidation, because the peak at 1580 cm^{-1} is due to aromatic C=C bond, and the peak at 1234 cm^{-1} is due to C—O bond [5,31]. The GO used in this study had the relative 1580/1234 cm^{-1} IR peak heights of 1.00/0.92, whereas a highly oxidized GO, prepared in our laboratory by Staudenmaier method [32], whose C/O ratio was 2.72/1.00, had the relative IR peak heights of 1.00/1.30. This also shows that the GO used in this study was moderately oxidized to have a proper conductivity.

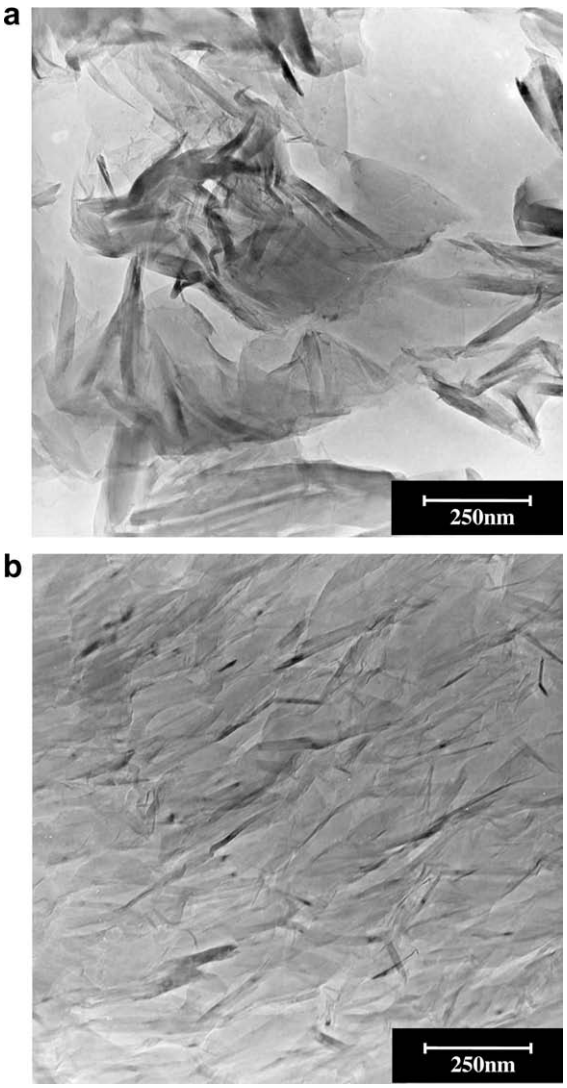

Fig. 2. TEM micrographs of GO/PMMA nanocomposites: (a) A-67, (b) B-67.

Table 2 shows that the conductivity of 10^{-5}–10^{-6} S/cm can be obtained with less than 5 parts of GO per 100 part of PMMA, and the conductivity of the B Series is much higher than that of the A Series. For example, the conductivity of B-25 is about 50-fold higher than that of A-25. This shows that the enhancement of conductivity by GO is much more effective when a fine dispersion was induced by exfoliation.

The polymerization yield and the molecular weight of matrix polymers analyzed by GPC are shown in Table 1 and Table 2, respectively. The polymerization yield was in the range of 80–90%. The matrix polymers of Series B have higher molecular weights than those of Series A. This shows that MAI, which has many azo groups linked by PEO blocks, can yield a larger multiblock copolymer having PMMA and PEO blocks by termination with a coupling reaction [33,34]. The GPC curves of B series had a shoulder because two kinds of initiators, MAI and AIBN, were used together.

The T_g values of GO/PMMA nanocomposites measured by DSC are shown in Table 2. This reveals that T_g increases more than 10 °C with a small amount of GO, even with less than 1 part per 100 parts PMMA, and these values increase further as the content of GO increases. In the nanocomposites, the T_g of matrix polymer generally increases compared to the pristine polymer because the segmental motions of the polymer chains are restricted at the filler-polymer interface due to filler-polymer interaction [35,36]. Thus, this T_g behavior supports the fact that GO is finely dispersed in the PMMA matrix in both Series A and Series B. The slightly higher T_g values of Series B compared to Series A at similar GO contents seem to be due to the finer dispersion caused by exfoliation as observed with TEM (Fig. 2).

The variations of storage tensile modulus (E') and *tan* δ of GO/PMMA nanocomposites from 50 to 220 °C are shown in Figs. 3 and 4. The E' values at 60 and 190 °C, and *tan* δ peak temperature, i.e., the T_g measured by DMA, are shown in Table 2, where it can be noted that E' generally increases as the content of GO is increased due to the reinforcing effect of GO. The E' values of fillers, GO in Series A and MAI/GO mixture (weight ratio; 1/5) in Series B, calculated with the following simple rule of mixture equation (Eq. (1)) are shown in Table 2. In Eq. (1), W is weight fraction, and the subscripts c, m and f refer to composite, matrix and filler, respectively. For the value of E'_m, the E' of A-0 at 60 °C was used. The average E'_f value GO in Series A was 11.5 GPa and that of GO/MAI in Series B was 7.0 GPa. When one considers that the in-plane and out-of-plane Young's moduli of graphite were suggested to be 600 and 10.5 GPa, respectively [37], it can be noted that moduli of GO in Series A or GO/MAI in Series B are similar to the out-of-plane Young's modulus of graphite. Since MAI generates N_2 during polymerization, GO/MAI in the composite is a mixture of GO and PEO block containing a small amount of residual ACPA fragments. This PEO block can soften and reduce the modulus of nanocomposite. On the other hand, the GO in Series B can reinforce the matrix poly-

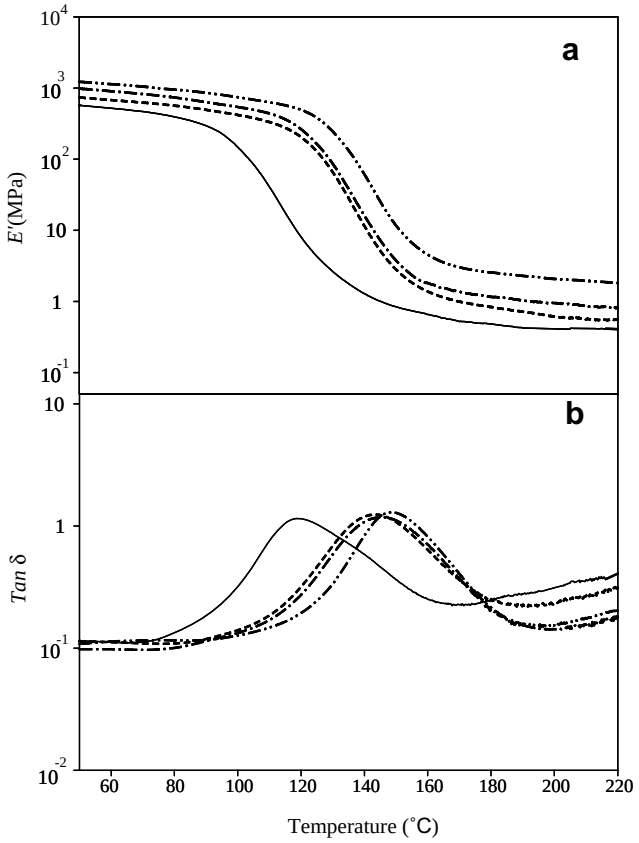

Fig. 3. Dynamic mechanical properties of (———) A-0, (– – – –) A-8, (— · — ·) A-42, (— · · —) A-67.

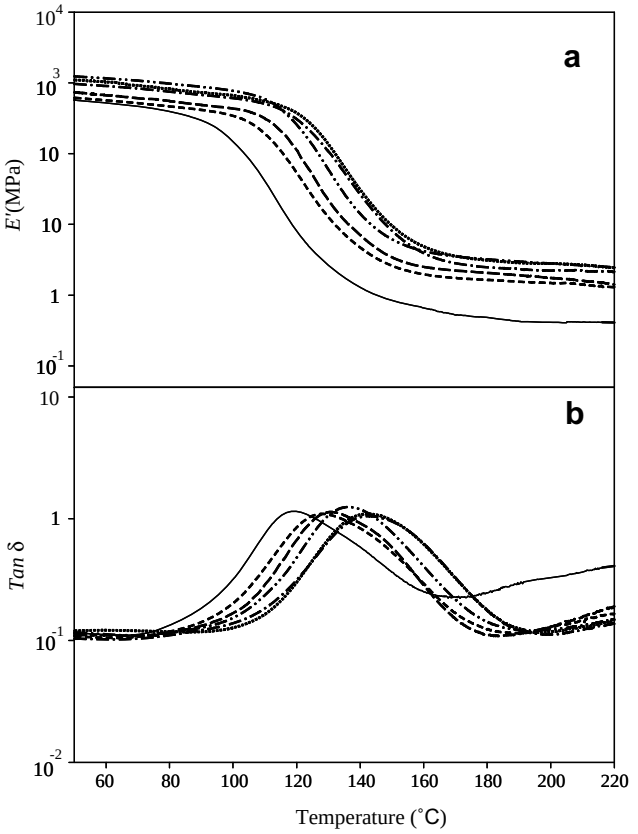

Fig. 4. Dynamic mechanical properties of (———) A-0, (– – – –) B-8, (— — —) B-17, (— · — ·) B-42, (·····) B-50, (— · · —) B-67.

mer more effectively compared to that of Series A because of exfoliation. Therefore, the smaller E'_f values of GO/MAI in Series B compared to those of GO in Series A show that the softening effect of PEO block is more predominant than the reinforcing effect by exfoliation.

$$E'_c = W_m E'_m + W_f E'_f \quad (1)$$

The T_g values of nanocomposites measured by DMA also generally increase as the content of GO is increased, as in the results measured by DSC (Table 2). However, when T_g was measured by DMA, the T_g values of Series B are generally lower than those of Series A at similar contents of GO, and B-67 has lower T_g compared to B-50. When one considers that external force is imposed for the measurement of DMA; whereas, there is no external force during the measurement by DSC, the above results suggest that softening due to heating can be accelerated by a soft PEO segment more evidently when external force is imposed, and this becomes distinct above a certain critical content of PEO.

4. Conclusions

The X-ray diffractograms and the morphologies observed by TEM show that the MAI intercalated in the gallery of GO effectively induced the inter-gallery polymerization to bring exfoliation, whereas the nanocomposites prepared with normal radical initiator, AIBN, had an intercalated structure.

The results of conductivity testing suggest that GO could be utilized effectively as a filler to improve the conductivity of PMMA, and this improvement was more evident in the exfoliated nanocomposites, showing a conductivity of 10^{-5} S/cm when 4.2 parts of GO were used per 100 parts of MMA.

The enhancement of E' and T_g, observed in both exfoliated and intercalated nanocomposites, indicates that GO efficiently reinforced the PMMA matrix.

Acknowledgements

This research was financially supported by the Ministry of Education, Science Technology (MEST) and Korean Industrial Technology Foundation (KOTEF) through the Human Resource Training Project for Regional Innovation.

References

[1] Cerezo FT, Preston CML, Shanks RA. Structural, mechanical and dielectric properties of poly(ethylene-co-methyl acrylate-co-acrylic acid) graphite oxide nanocomposites. Compos Sci Technol 2007;67:79–91.
[2] Kalaitzidou K, Fukushima H, Drzal LT. A new compounding method for exfoliated graphite-polypropylene nanocomposites with enhanced flexural properties and low percolation threshold. Compos Sci Technol 2007;67:2045–51.
[3] Lei SG, Hoa SV, Ton-That M-T. Effect of clay types on the processing and properties of polypropylene nanocomposites. Compos Sci Technol 2006;66:1274–9.
[4] Jeong H-K, Lee YP, Lahaye RJWE, Park M-H, An KH, Kim IJ, et al. Evidence of graphitic AB stacking order of graphite oxides. J Am Chem Soc 2008;130:1362–6.
[5] Szabó T, Berkesi O, Forgó P, Josepovits K, Sanakis Y, Petridis D, et al. Evolution of surface functional groups in a series of progressively oxidized graphite oxides. Chem Mater 2006;18:2740–9.
[6] Lerf A, He H, Forster M, Klinowski J. Structure of graphite oxide revisited. J Phys Chem B 1998;102:4477–82.
[7] Wang J, Han Z. The combustion behavior of polyacrylate ester/graphite oxide composites. Polym Adv Technol 2006;17:335–40.

[8] Hua L, Kai W, Inoue Y. Synthesis and characterization of poly(ε-caprolactone)-graphite oxide composites. J Appl Polym Sci 2007;106:1880–4.
[9] Uhl FM, Wilkie CA. Preparation of nanocomposites from styrene and modified graphite oxides. Polym Degrad Stab 2004;84:215–26.
[10] Wang W-P, Pan C-Y. Preparation and characterization of poly(methyl methacrylate)-intercalated graphite oxide/poly(methyl methacrylate) nanocomposite. Polym Eng Sci 2004;44:2335–9.
[11] Higashika S, Kimura K, Matsuo Y, Sugie Y. Synthesis of polyaniline-intercalated graphite oxide. Carbon 1999;37:351–8.
[12] Wang G, Yang Z, Li X, Li C. Synthesis of poly(aniline-co-*o*-anisidine)-intercalated graphite oxide composite by delamination/reassembling method. Carbon 2005;43:2564–70.
[13] Dutta K, De SK. Electrical conductivity and optical properties of polyaniline intercalated graphite oxide nanocomposites. J Nanosci Nanotechnol 2007;7:2459–65.
[14] Bissessur R, Liu PKY, Scully SF. Intercalation of polypyrrole into graphite oxide. Synth Met 2006;156:1023–7.
[15] Jeong HM, Choi MY, Ahn YT. Morphology and properties of polyacrylonitrile/Na-MMT nanocomposites prepared via in-situ polymerization with macroazoinitiator. Macromol Res 2006;14:312–7.
[16] Weimer MW, Chen H, Giannelis EP, Sogah DY. Direct synthesis of dispersed nanocomposites by in situ living free radical polymerization using a silicate-anchored initiator. J Am Chem Soc 1999;121:1615–6.
[17] Matsuo Y, Watanabe K, Fukutsuka T, Sugie Y. Characterization of *n*-hexadecylalkylamine-intercalated graphite oxides as sorbents. Carbon 2003;41:1545–50.
[18] Liu P, Gong K, Xiao P. Preparation and characterization of poly(vinyl acetate)-intercalated graphite oxide. Carbon 1999;37:2073–5.
[19] Matsuo Y, Tahara K, Sugie Y. Synthesis of poly(ethylene oxide)-intercalated graphite oxide. Carbon 1996;34:672–4.
[20] Matsuo Y, Tahara K, Sugie Y. Structure and thermal properties of poly(ethylene oxide)-intercalated graphite oxide. Carbon 1997;35:113–20.
[21] Xu J, Hu Y, Song L, Wang Q, Fan W, Chen Z. Increasing the electromagnetic interference shielding effectiveness of carbon fiber polymer-matrix composite by using activated carbon fibers. Carbon 2002;40:445–7.
[22] Kovtyukhova NI, Ollivier PJ, Martin BR, Mallouk TE, Chizhik SA, Buzaneva EV, et al. Layer-by-layer assembly of ultrathin composite films from micron-sized graphite oxide sheets and polycations. Chem Mater 1999;11:771–8.
[23] Kyotani T, Moriyama H, Tomita A. High temperature treatment of polyfurfuryl alcohol/graphite oxide intercalation compound. Carbon 1997;35:1185–7.
[24] Ueda A, Nagai S. Block copolymers derived from azobiscyanopentanoic acid. VI. Synthesis of a polyethylene glycol-polystyrene block copolymer. J Polym Sci Polym Chem 1986;24:405–18.
[25] Hontoria-Lucas C, López-Peinado AJ, López-González J, Rojas-Cervantes ML, Martín-Aranda RM. Study of oxygen-containing groups in a series of graphite oxides: physical and chemical characterization. Carbon 1995;33:1585–92.
[26] Hamwi A, Marchand V. Some chemical and electrochemical properties of graphite oxide. J Phys Chem Solids 1996;57:867–72.
[27] Morgan AB, Gilman JW. Characterization of polymer-layered silicate (clay) nanocomposites by transmission electron microscopy and X-ray diffraction: a comparative study. J Appl Polym Sci 2003;87:1329–38.
[28] Szabó T, Tombácz E, Illés E, Dékány I. Enhanced acidity and pH-dependent surface charge characterization of successively oxidized graphite oxides. Carbon 2006;44:537–45.
[29] Stankovich S, Piner RD, Chen X, Wu N, Nguyen ST, Ruoff RS. Stable aqueous dispersions of graphitic nanoplatelets via the reduction of exfoliated graphite oxide in the presence of poly(sodium 4-styrenesulfonate). J Mater Chem 2006;16:155–8.
[30] Staukovich S, Dikin DA, Dommett GHB, Kohlhaas KM, Zimney EJ, Stach EA, et al. Graphene-based composite materials. Nature 2006;442:282–6.
[31] Du X, Yu Z-Z, Dasari A, Ma J, Mo M, Meng Y, et al. New method to prepare graphite nanocomposites. Chem Mater 2008;20:2066–8.
[32] McAllister MJ, Li J-L, Adamson DH, Schniepp HC, Abdala AA, Liu J, et al. Single sheet functionalized graphene by oxidation and thermal expansion of graphite. Chem Mater 2007;19:4396–404.
[33] Kim MS, Jun JK, Jeong HM. Shape memory and physical properties of poly(ethyl methacrylate)/Na-MMT nanocomposites prepared by macroazoinitiator intercalated in Na-MMT. Compos Sci Technol 2008;68:1919–26.
[34] Inoue H, Ueda A, Nagai S. Block copolymers derived from azobiscyanopentanoic acid. X. Synthesis of silicone-vinyl block copolymers via polysiloxane(azobiscyanopentanamide)s. J Polym Sci Polym Chem 1988;26:1077–92.
[35] Jeong HM, Choi MY, Kim MS, An JH, Jung JS, Kim JH, et al. Styrenic polymer/organoclay nanocomposite prepared via in-situ polymerization with an azo initiator linked to an epoxy oligomer. Macromol Res 2006;14:610–6.
[36] Uthirakumar P, Nahm KS, Hahn YB, Lee Y-S. Preparation of polystyrene/montmorillonite nanocomposites using a new radical initiator-montmorillonite hybrid via in situ intercalative polymerization. Eur Polym J 2004;40:2437–44.
[37] Yasmin A, Daniel IM. Mechanical and thermal properties of graphite platelet/epoxy composites. Polymer 2004;45:8211–9.